Steel and Composite Structures, *Vol. 36, No. 4* (*2020*) *417-426*
DOI: https://doi.org/10.12989/scs.2020.36.4.417

Analysis of the machinability of GFRE composites in drilling processes

Usama. A. Khashaba[1,2], Mohamed S. Abd-Elwahed[1], Khaled I. Ahmed[1], Ismail Najjar[1], Ammar Melaibari[1] and Mohamed A Eltaher *[1,2]

[1]*Mechanical Engineering Department, Faculty of Engineering, King Abdulaziz University, P.O. Box 80204, Jeddah 22254-2265, Saudi Arabia*
[2]*Mechanical Design and Production Engineering Department, Faculty of Engineering, Zagazig University, Egypt*

(*Received May 17, 2020, Revised July 29, 2020, Accepted July 30, 2020*)

Abstract. Drilling processes in fiber-reinforced polymer composites are essential for the assembly and fabrication of composite structural parts. The economic impact of rejecting the drilled part is significant considering the associated loss when it reaches the assembly stage. Therefore, this article tends to illustrate the effect of cutting conditions (feed and speed), and laminate thickness on thrust force, torque, and delamination in drilling woven E-glass fiber reinforced epoxy (GFRE) composites. Four feeds (0.025, 0.05, 0.1, and 0.2 mm/r) and three speeds (400, 800, and 1600 RPM) are exploited to drill square specimens of 36.6x36.6 mm, by using CNC machine model "Deckel Maho DMG DMC 1035 V, ecoline". The composite laminates with thicknesses of 2.6 mm, 5.3 mm, and 7.7 mm are constructed respectively from 8, 16, and 24 glass fiber layers with a fiber volume fraction of about 40%. The drilled specimen is scanned using a high-resolution flatbed color scanner, then, the image is analyzed using CorelDraw software to evaluate the delamination factor. Multi-variable regression analysis is performed to present the significant coefficients and contribution of each variable on the thrust force and delamination. Results illustrate that the drilling parameters and laminate thickness have significant effects on thrust force, torque, and delamination factor.

Keywords: drilling of composite; woven glass fiber; thrust force and torque; delamination, Multiple Regression

1. Introduction

Polymeric composite materials have been grown into a significant part of everyday life due to their superior multifunctional properties and lightweight characteristics. The application spectrum of these materials includes aerospace and automotive industries, sports goods, housing and gardening equipment, consumer products, tissue engineering, orthopedics, and dental implants and others, Debnath (2019), Hamed *et al*. (2020). Laminated composite structures are made-up of composite materials plies with desirable angle orientations to accomplish desirable and high-performance mechanical properties, Eltaher and Mohamed (2020). The fuel savings and higher specific strength/stiffness offered by lightweight FRP composites make them attractive for commercial airplanes, military aircraft, and automotive industries. For example, the used fiber composites in Boeing 787 Dreamliner and the Airbus A350 XWB was more than 50% of wings, tail surfaces, and fuselage sections, Khashaba (2020). In these applications, drilling holes are essential for the repair of composite structures and in the assembly/fabrication of new aircraft. Airbus company as one of the leaders of aircraft manufacturing produced over 120 million holes for assembling 630 A320 Family aircraft in 2016, Hrechuk *et al*. (2018). Hole quality usually is the limiting factor in the assembly of the composite structure and thus, is considered one of the main goals in drilling FRP composites.

Drilling, which is a commonly applied hole machining procedure, is an almost unavoidable operation for assembly, joining, and repairing of real applications manufactured by composite structures, Khashaba and Khdair (2017). Drilling holes can lead to many defects in composites, such as interlaminar debonding (delamination) between two adjacent plies, fiber pull-out or breakage, matrix cracking, or thermal degradation. In the aircraft industry, poor-quality holes account for an estimated 60% of all disqualified CFRP parts. Therefore, the effect of drilling-induced delamination on the CFRP must necessarily to be considered in the damage tolerance design of aircraft for the effective reduction of costs, Haeger *et al*. (2016).

Nowadays, the effect of drilling parameters on the thrust force, torque, and delamination of composite structures gains a lot of researchers and scientists' scope. Khashaba (2004) proved experimentally that chopped composites have lower push-out delamination than those made from woven fibers and for the same fiber shape, the peel-up and push-out delaminations of woven/epoxy composite are lower than that for woven/polyester composites. In drilling chopped composites, Khashaba *et al*. (2007) concluded that the push-out delamination is more severe than peel-up delamination for the same-drilled hole, and the cutting speed has no clear effect on the delamination size. Wang *et al.* (2009) developed a simple method to detect the bonding condition of active fiber composites (AFC) adhered to the surface of a host structure. Liu *et al.* (2012) and Khashaba

*Corresponding author, Professor
E-mail: meltaher@kau.edu.sa

Copyright © 2020 Techno-Press, Ltd.

ISSN: 1229-9367 (Print), 1598-6233 (Online)

(2013) presented a comprehensive review in the drilling of composite covers drilling operations, drill bit geometry and materials, drilling-induced delamination, thrust force, and tool wear. Rakesh *et al.* (2012) suggested drilling damage-free holes in composite by using modified four different drill geometries (solid and hollow in shape) for drilling. Khashaba *et al*. (2013) investigated the effects of drilling parameters on the machinability parameters in drilling woven glass fiber-reinforced at high feeds (0.45 mm/rev). Phadnis *et al*. (2013) studied experimentally and numerically effects of cutting parameters on drilling thrust force and torque during the machining process of carbon fiber reinforced plastics (CFRPs). Kharazan *et al*. (2014) investigated delamination growth in composite laminates subjected to low-velocity impact. Zemirline *et al*. (2015) studied the dynamic behavior of piezoelectric bimorph beams with a delamination zone by using the finite element method. Mahieddine *et al*. (2015) presented modeling and simulation of partially delaminated composite beams by using first-order shear deformation theory. Kumar *et al*. (2016) studied experimentally delamination and surface roughness induced by drilling of glass fiber composite material with different drills and predicted that qualities of drill holes significantly improved when solid carbide eight-facet drill was used. Bin Kamisan *et al*. (2016) investigated drilling force and speed for mandibular trabecular bone in oral implant surgery. Biswal *et al.* (2016) experimentally studied the critical loads of laminated composite cylindrical shell panels that are made of hygrothermal treated woven fiber-glass/epoxy by using a universal testing machine INSTRON 8862.

Khashaba and El-Keran (2017) explored experimentally and analytically the thrust force and the delamination of thin woven glass-fiber-reinforced epoxy composites in the drilling process. Achache *et al*. (2017) studied the delamination of a composite laminated under monotonic loading. Moory- Fazilati (2018) investigated the parametric instability characteristics of tow-steered variable stiffness composite laminated cylindrical panels using the B-spline finite strip method considering geometrical defects including cutout and delamination. Geng *et al.* (2019) presented a review on the formation and evaluation of delamination created during drilling of composite laminates. Gemi *et al.* (2019a) studied experimentally the impact of drill types on the drilling performance of glass fiber composite pipes and damage formation. Gemi *et al.* (2019b, 2020) studied the effects of stacking sequence of filament wound hybrid composite pipes on mechanical characterization, damage, and surface quality through the drilling process. Dehghan and Heidary (2020) and Heidary *et al*. (2020) examined the influences of drilling parameters and drill geometry on the thrust force and the delamination factor for the composite pipes produced by the filament winding process. Rahme *et al.* (2020) explored the influence of adding a woven glass ply at the exit of the hole of CFRP laminates on delamination during the drilling process.

Based on analytical and numerical methods, Chandrasekharan *et al*. (1995) developed models to predict the thrust and torque forces at the different regions of cutting on a drill exploits the geometry of the process, which is independent of the workpiece material. Bui (2011) exploited the linear fracture criterion to modified the Benzeggagh-Kenane fracture criterion for mixed-mode delamination. Sedighi *et al*. (2014, 2015) investigated non-linear dynamic instability of a double-sided nano-bridge considering centrifugal force and rarefied gas flow. Sedighi and Bozorgmehri (2016) studied the dynamic instability of doubly clamped cylindrical nanowires in the presence of Casimir attraction and surface effects using a modified couple stress theory. Based on elastic fracture mechanics, classical plate bending theory and the mechanics of oblique cutting, Karimi *et al.* (2016) developed analytical models to predict critical thrust force and feed rate at the onset of delamination. Ojo *et al*. (2017) and Heidary and Mehrpouya (2019) developed analytical models to predict the critical thrust force and the feed rate for drilling of composite laminates with a backup plate. Ouakad and Sedighi (2017) studied nonlinear internal resonances of a microelectromechanical systems arch when excited by static (DC) and dynamic (AC) electric forces. Taheri-Behrooz *et al.* (2018) evaluated residual stresses in the butt joint welded metals using friction stir welding and tungsten inert gas methods. Shirbani *et al.* (2018) presented an experimental and mathematical analysis of a piezoelectrically actuated multilayered imperfect microbeam subjected to applied electric potential. Ghosh and Chakravorty (2019) used the finite element method to predict failure on the first ply of composite hyper shells with various edge conditions. Beylergil *et al*. (2019) showed that the propagation Mode-I fracture toughness values of carbon fiber/epoxy (CF/EP) composites can be significantly improved (by about 72%) using aramid nonwoven fabrics. Díaz-Álvarez *et al*. (2019) analyzed the influence of the point angle of the drill on the generated damage during drilling of a biodegradable composite. Baraheni *et al.* (2019) developed a parametric analysis of delamination in glass fiber composite profiles generated by an unconventional rotary ultrasonic drilling approach. Xu *et al.* (2019) presented an accurate model to identify the delamination of laminated composite plates using measured mode shapes. Bhat (2019) presented multi-response optimization of the thrust force, torque, and surface roughness in the drilling of glass fiber reinforced polyester composite. Mousavi and Yazdi (2019) investigated the effect of carbon nanotubes (CNTs) on critical flutter pressure of reinforced damaged nano-composite structures such as delamination. Eltaher and Abdelrahmaan (2020) and Almitani (2020) studied the bending and buckling of perforated nanobeam with surface energy effects. Melaibari *et al.* (2020) studied the static stability of symmetric and sigmoid functionally graded beam under variable axial load. Mishra *et al*. (2020) developed a numerical simulation model to present the influence of residual thermal stresses and material anisotropy on the inter-laminar delamination behavior of the joint structure.

Corresponding to the authors' knowledge and literature survey, the influence of drilling parameters (feed and speed) on thrust force, torque, and delamination of woven glass fiber composite has not been investigated at different

specimen thicknesses with a high accuracy CNC machine. So, this article fills this gap and presents an experimental analysis of thrust force and damage in the drilling of glass fiber composites. The tested composite laminates are locally fabricated. Peel-up and push-out delaminations are measured using the AutoCAD technique that was developed by Khashaba (2004). The thrust force and torque are measured through standard set-up using the Kistler dynamometer model 9272 fixed on a CNC milling machine. The article is organized as follows:- experimental work including specimen preparation, mechanical testing, and drilling operation are illustrated in section 2. Section 3 is devoted to the present impacts of drilling parameters on thrust force, torque, and delamination of the holed specimen. Multi-variable regression analysis is presented in section 4. Conclusions and main points are summarized in section 5.

2. Experimental work

2.1 Specimen preparation

The hand lay-up technique is used to manufacture three groups of woven E-glass fiber reinforced epoxy (GFRE) composite laminates with different thicknesses and layers. The composite laminates with thicknesses of 2.6 mm, 5.3 mm, and 7.7 mm (± 0.12 mm) are constructed respectively from 8, 16 and, 24 glass fiber layers, epoxy matrix Araldite LY5138-2, and Hardener HY5138. The fiber volume fraction (V_f) of the fabricated laminates is calculated from the number of layers (n), the areal weight of the fabric (A_w), the thickness of the product (t), and the fiber density (ρ_f), using Eq. (1) , Ouagne *et al.* (2013). The results are illustrated in Table 1.

$$V_f = \frac{n A_w}{\rho_f t} \quad (1)$$

2.2 Mechanical testing

The test specimens are cut to the standard dimension using CNC abrasive water-jet machine to eliminate any generated heat effects that might be produced with conventional machining processes. The tensile properties of the fabricated materials are characterized according to ASTM D 3039 using the servo-hydraulic testing machine model Instron 8803 (500kN). The specimens are loaded at a test rate of 1.0 mm/min. The tensile specimens are equipped by two perpendicular strain gauges at the center of the gauge length (170 mm) to determine the true elastic properties (modulus and Poisson's Ratio) of the fabricated materials. The longitudinal and transverse strains are measured using 4-channel data acquisition model 9237 NI. Five specimens are tested for each laminate thickness and the average values are tensile strength of 203.86 MPa, the elastic modulus of 16.05 GPa, and Poisson's ratio of 0.295.

Table 1 The estimated fiber volume fraction of the fabricated GFRE laminates

n (Layers)	A_w (g/m^2)	ρ_f (g/cm^3)	t (mm)	V_f (%)
8	324	2.5	2.59	40.0
16	324	2.5	5.25	39.5
24	324	2.5	7.73	40.2

2.3 Drilling operations

Drilling processes are implemented under dry cutting conditions using a CNC milling machine model "Deckel Maho DMG DMC 1035 V, Ecoline". The CNC machine can perform the drilling process at cutting speeds up to 10,000 RPM. Two flute drills are manufactured from special ultra-fine cemented carbide tip, which is used for efficient cutting, with excellent toughness and abrasion resistance. Details about the constituent materials of the twist drill are presented in Table 2. The drills have the following geometrical parameters: d = 6 mm, flute length = 28 mm, overall length = 66 mm, point angles, ϕ = 100 °, helix and rake angles = 30°, clearance angle = 12 °, chisel edge length= 0.3 mm. The drilling processes are performed at cutting speeds of 400 RPM (7.5 m/min), 800 RPM (15 m/min), and 1600 RPM (30 m/min). Four feeds of 0.025, 0.05, 0.1 and 0.2 mm/r are applied. The cutting conditions are selected in similar ranges used by many researchers [Hocheng *et al.* (2018), Heidary and Mehrpouya (2019), Feito *et al.* (2019) and, Prasad and Chaitanya (2019)]. Higher feeds are expected to increase the thrust force and thus the mechanical damages such as the push-out delamination. Drilling at high cutting speeds is expected to increase the induced temperature and thus, the thermal damage such as burning the matrix and degrading the bearing strength of the heat-affected zone.

Based on the literature and the present work, the measured machinability parameters in drilling FRP have a high level of repeatability. Therefore, the drilling process is repeated just twice for each condition. However, three specimens are used in some cases, which have shown minor deviations. The drilling processes are performed on square specimens of 36.6x36.6 mm, which are cut using an abrasive water jet machine. The specimen dimensions are selected per ASTM D 5961 that enables the authors to perform pure bearing tests in the following research work. Fig. 1 illustrates the experimental setup for online measuring thrust and torque and the dynamometer-fixture-workpiece assembly. Kistler dynamometer model 9272 that can measure thrust force and torque up to 20 kN and 200 N.m respectively is used. The specimen is fixed on the dynamometer via a circular aluminum disk with U-grove. The disk is clamped on the specimen using two-bolts (M-16). The back-up plate has a hole on the exit of 20-mm diameter. As noted in Figure a very weak GFRE composite chip is attached to the drill.

Table 2. The constituent materials of the cemented carbide drills

Material grade	ISO code	WC	Co	Grain size	Proportion	Hardness	Flexural strength
K200	K20~K40	90%	10%	0.5~0.8 µm	14.4 g/cm^3	91.3	3923 MPa

Fig. 1 (a) Experimental setup for online measuring thrust and torque on CNC milling model Deckel Maho DMG DMC 1035 V and (b) enlarged view of the dynamometer-fixture-workpiece assembly

3. Results and discussion

This section presents the influences of cutting speed and feed on the thrust force, torque, and delamination in drilling of GFRE composite with different thicknesses. Examples of the induced delamination images in drilling GFRE composites are illustrated in Fig. 2 for different feed and a speed of 800 rpm. The images are scanned using a high-resolution flatbed color scanner model Epson "V370, 4800 x 9600 dpi". The variation of thrust force concerning displacement and time during drilling of woven GFRE composite at a speed of 800 RPM and a 0.1 mm/ rev feed for a specimen with 7.7 mm thickness is shown in Fig. 3. The data are recorded with frequency =1000 Hz and filtered at 100 data points.

As noticed in Fig. 3, four different stages are observed for the thrust force-displacement/time that is portrayed as follows:

In the first stage (stage I) at the entry of the chisel edge into the workpiece, the thrust force is increased sharply in a linear behavior. This behavior represents the elastic loading of the workpiece owing to the negative rake angle of the chisel edge accompanied by its zero-center speed. Therefore, the chisel edge will push-out (extrude) the materials instead of cutting it.

The second stage (stage II) begins when the chisel edge penetrates the workpiece surface layer. At this instant, the thrust force increases linearly with peaks and valleys up to the maximum value of thrust force.

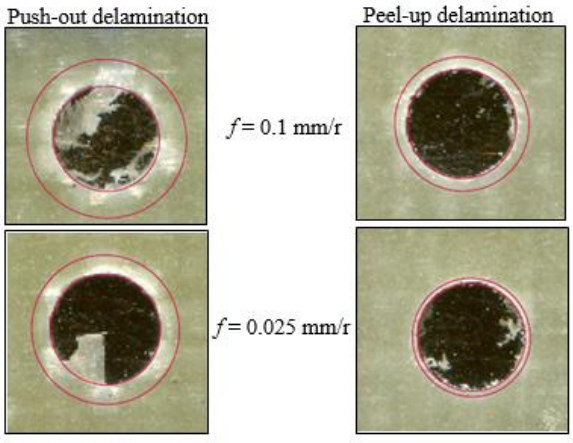

Fig. 2 Examples for peel-up and push-out delaminations at different feeds and a speed of 800 rpm (Delamination ratio = D_{max}/D_0)

the form of peaks and valleys are observed when the cutting edge enters a new layer (uncut-chip area increases) and the remaining uncut layers in front of the chisel edge are decreased by one. The maximum thrust force is observed when the drill edge is completely engaged with the specimen.

The third stage (stage III) is started from the complete engaged of the drill with the specimen until the edge of the drill just exits through the specimen. In this stage, the thrust force is decreased gradually due to a reduction in stiffness of the specimen that is caused by the removal of material under the drill. Also, softening the polymer composites due to the induced temperature is another reason for decreasing the thrust force, Khashaba (2013).

The fourth stage (stage IV) starts when the chisel edge of the drill just exits the specimen causing a higher reduction in thrust force by about 50%. Then gradual reduction in the thrust force is observed up to the end of the drilling cycle due to the gradual exit of the two cutting edges of the drill. It is worth noting that, in *stage II* the increase in the thrust force due engagement of the cutting edges is about 35 N at 2.5 mm, which equals the drop in the thrust force in *stage IV* (in about 2.5 mm).

The effect of speed and feed on the maximum thrust force and torque for different thicknesses and layers are presented in Figs. 4 and 5. It is noted from Fig. 3 that at a specified thickness, the thrust load decreases with a small linear rate as the speed increases. At cutting speed of 1600 rpm, the maximum thrust load decreases by a maximum of 15%. However, in most cases, this reduction is less than 15%. So, the thrust force is proportional inversely with speed. It is clear from Fig. 3 that the higher the feed the higher the thrust load. So, the feed has a proportional significant effect on the thrust load. It is evident from Fig. 3 that the feed has the most significant effect on the thrust load compared to the effect of cutting speed.

By comparing the maximum thrust force for the three different thicknesses, it is noted that the thicknesses of 5.3 and 7.7 have a marginal effect on the thrust force. The smallest specimen thickness has the lowest thrust force. This result is attributed to the exit of the chisel edge from the specimen before full engagement of the cutting edges. The height of the drill point equal $(d/2)/\tan(\phi/2) = 2.52$ mm, which is approximately equal to the laminate thickness of 2.6 ± 0.12 mm.

The effects of feed, speed, and specimen thickness on the torque are presented in Figs. 5(a)-5(c). It is noted that these effects have the same behavior as the maximum thrust force. Increasing the thickness from 5.3 to 7.7 has a significant effect on the torque rather than thrust force. This is attributed to the friction increase between the machined surface, chip, and drill flanks.

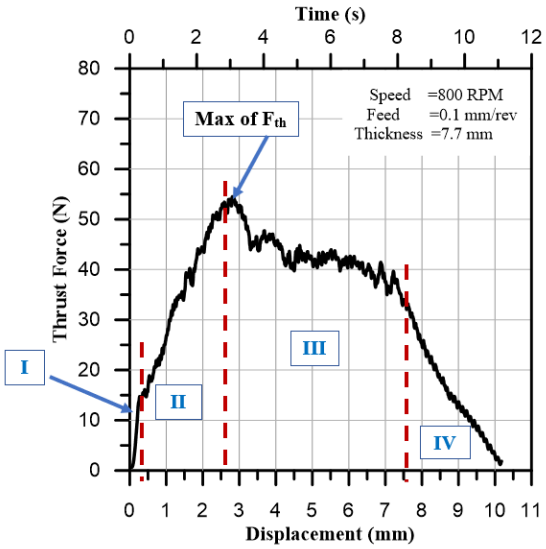

Fig. 3 Thrust force over drilling cycle of GFRE composite at 800 RPM and 0.1 mm/rev feed for a specimen with 7.7 mm thickness and 24 layers

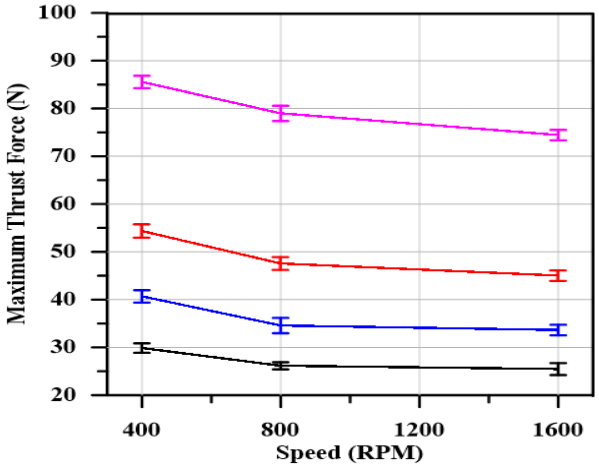

(a) Thickness =2.6 mm

Continued-

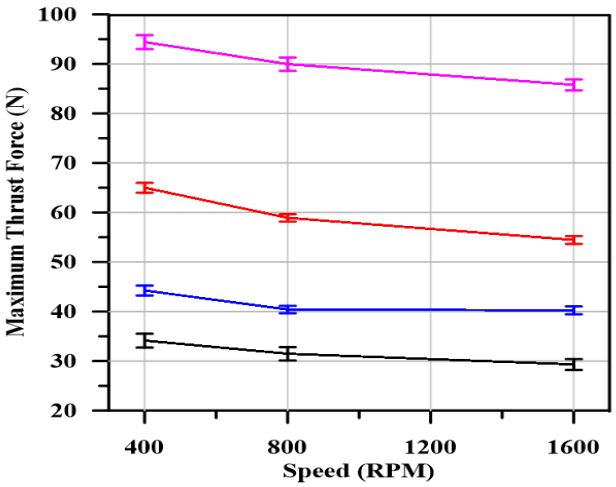

(b) Thickness =5.3 mm

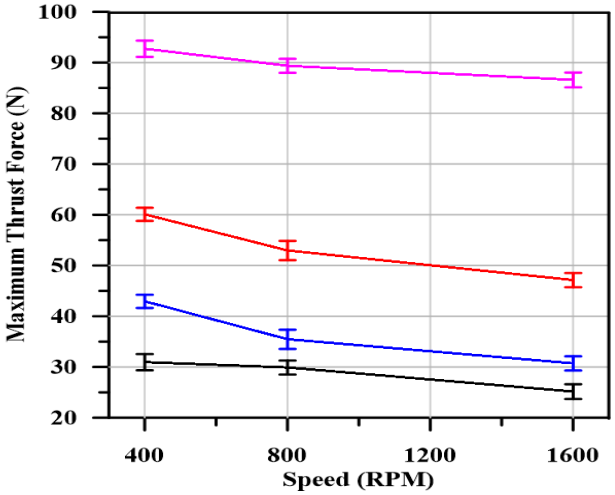

(c) Thickness =7.7 mm

Fig. 4 Influences of speed and feed on maximum thrust force at different thicknesses and number of layers

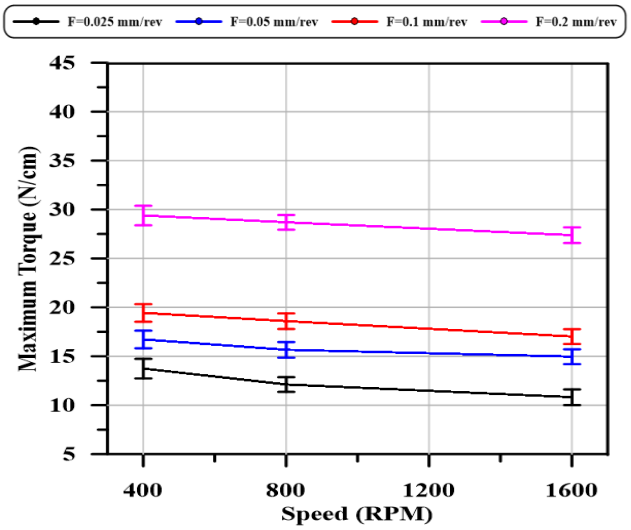

(a) Thickness =2.6 mm

Continued-

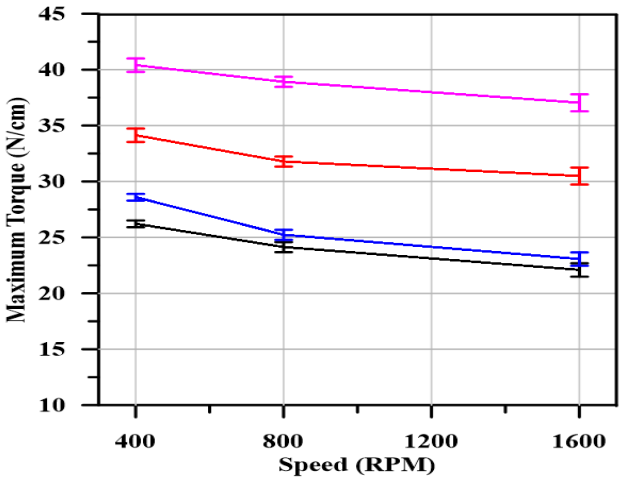

(b) Thickness =5.3 mm

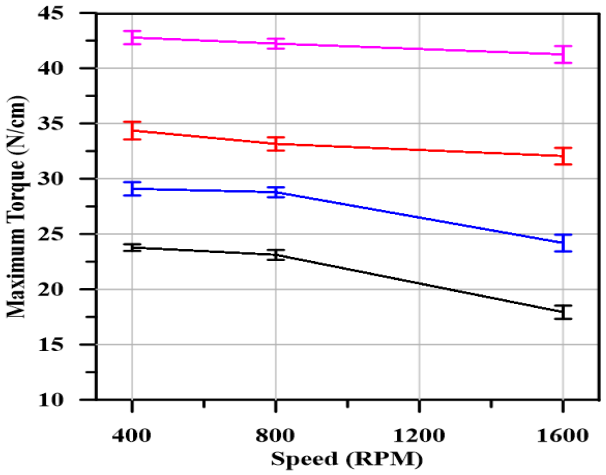

(c) Thickness =7.7 mm

Fig. 5 Influences of speed and feed on maximum torque at different thicknesses and number of layers

The effects of feed and thickness on delamination are presented in Fig. 6. As shown, peel up and push out delamination are increased significantly by increasing the cutting feed. The push-out delamination is higher than peel-up. As the thickness increases, the delamination decreases as presented in Fig. 6.

4. Multi-variable regression analysis

In the last few years, considerable attention has been paid to record the multiple regression models that correlate machinability parameters with machining conditions in drilling fiber-reinforced composites Khashaba (2010), Agwa and Megahed (2019). Design of Experiment methods (DOE) have been used extensively in investigating the significance of cutting conditions factors on the delamination of fiber composites during the drilling process. Kilickap (2010) presented a review on the applicability of the Taguchi method in the optimization of cutting parameters on delamination during drilling of glass fiber composite. Sedighi *et al.* (2012a, b) used a parameter expansion method to obtain the exact solution of the

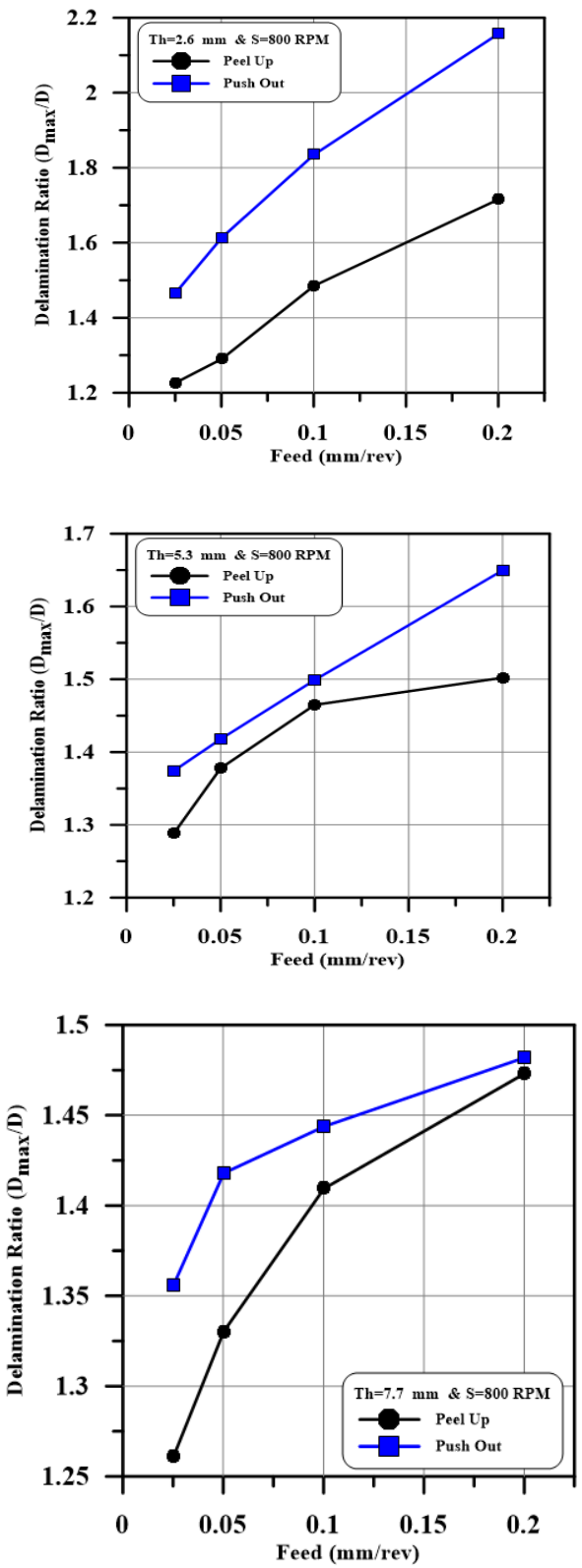

Fig. 6 Effects of feed and thickness on peel up and push out delamination

dynamic behavior of a buckled beam. Krishnaraj *et al.* (2012) presented an experimental investigation of a full factorial design performed on thin CFRP laminates using K20 carbide drill by varying the drilling parameters by

using Analysis of variance (ANOVA) and Genetic Algorithm (GA). Yun and Abdel Wahab (2017) detected damage of composite structures using vibration data and dynamic transmissibility ensemble with an auto-associative neural network. Nguyen *et al*. (2019) predicted damage in a girder bridge using transmissibility functions as input data to Artificial Neural Networks. Tran-Ngoc *et al*. (2019) discovered a failure in bridges and beam-like structures by improving the training parameters of artificial neural networks using a cuckoo search algorithm. Khatir et al. (2019, 2020) improved the artificial neural networks technique combined with the Jaya algorithm for crack identification in plates using eXtended IsoGeometric Analysis and experimental analysis.

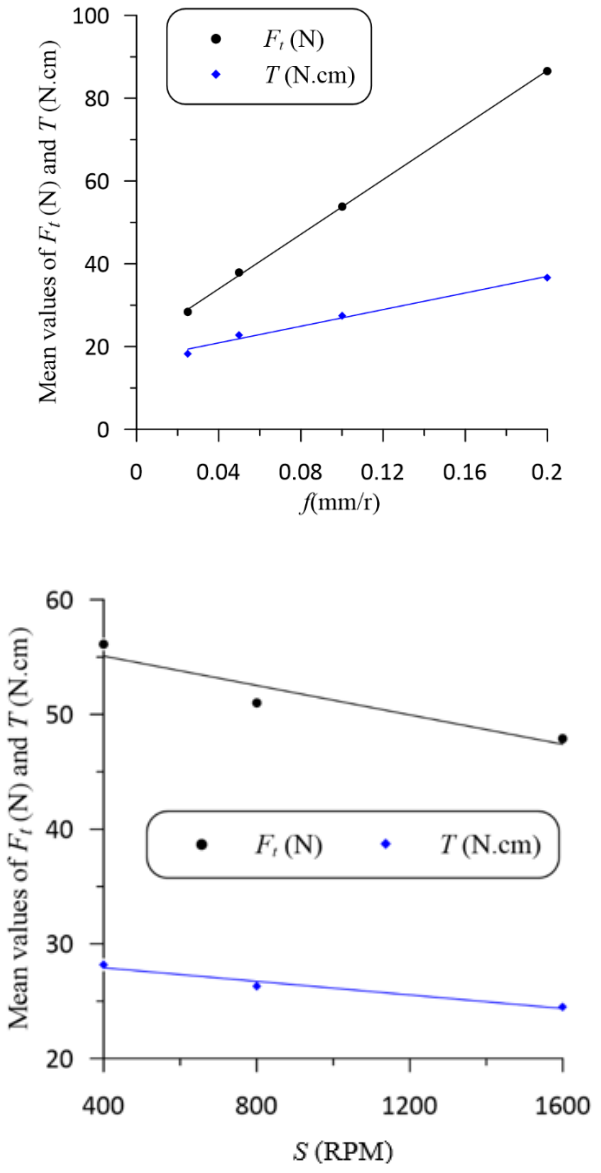

Fig. 7 Predicted mean values of F_t and T using Eqs. (2) and (3) respectively (a) vs feed and (b) vs speed

In the present work multiple linear regression models are developed to correlate the machinability parameters: thrust force, F_t (N), torque, T (N.cm), feed, f (mm/r), speed, s (rpm), and specimen thickness t (mm). The correlations between the machinability parameters (F_t and T) and drilling variables f, v, and t can be represented as follows

$$F_t = 14.11 + 276.0\ f - 0.01766\ S + 8.492\ t - 138\ f^2 - 0.8615\ t^2 - 0.0045\ f\ S + 10.40\ f\ t \quad (2)$$

$$T = -6.21 + 116.7f - 0.003798S + 8.856t - 256.6f^2 - 0.6764t^2 + 0.01884f\ S + 4.83f\ t \quad (3)$$

The multiple coefficients of correlation (R^2) are 0.990 and 0.976 for F_t and T respectively.

The values of regression coefficients (R^2) indicate that the multivariable regression models are very good to fit the experimental data of machinability parameters. It is worth noting that, Tsao and Hocheng (2008) developed a linear regression model for prediction thrust force in drilling carbon fiber/epoxy composites with R^2 = 0.81. Figs. 7(a) and 7(b) show the predicted mean values of F_t (N) and T (N.cm) versus feed (mm/r) and speed (rpm) respectively. It is worth noting that the predicted mean thrust force and torque are increased by 204.9% and 100% respectively with an increase of the feed from 0.025 to 0.2 mm/r. On the other hand, the predicted mean thrust force and torque are decreased by 16.6% and 13.1 % respectively with an increase of the feed from 0.025 to 0.2 mm/r.

5. Conclusions

This work investigates the effect of machining parameters on thrust force, torque, and delamination in drilling woven E-glass fiber reinforced epoxy (GFRE) composites. The main conclusion points can be summarized as:

- The feed has highly significant effects on the thrust force, torque, and delamination. They are increased by increasing the feed. The thrust force increased 3 times as the feed increase from 0.025 to 0.2 mm/r.
- The thrust force and torque are proportional inversely with the speed of drilling. However, the speed effects are not highly pronounced. At cutting speed of 1600 rpm, the maximum thrust load decreased by 15% as a maximum. In most cases, this reduction is less than 15%.
- The push out delamination is higher than the peel up delamination. The push out delamination increased by a range of 3.4% - 30% relative to peel up delamination.
- The predicted mean thrust force and torque using the Multi-Variable Regression model are increased by 204.9% and 100% respectively with an increase of the feed from 0.025 to 0.2 mm/r. On the other hand, the predicted mean thrust force and torque are decreased by 16.6% and 13.1 % respectively with an increase of the feed from 0.025 to 0.2 mm/r.
- Increasing the thickness of the composite laminate leads to increasing the cutting time and thus the

induced temperature in the drilling process. Increasing the temperature is assisted by the poor thermal conductivity of GFRP composites which is very low (0.59 W/m℃) compared to steel (= 53 W/m℃), brass (= 109 W/m℃), and Aluminum (= 210 W/m℃). The temperature increase has conflict effects on the machinability parameters. Increasing the temperature to some extent can lead to softening the specimens and thus, reduce thrust force, the moment of friction force on the margins, and the mechanical damages. On the other hand, thermal damage such as burning the matrix can be observed at elevated temperatures. Therefore, the following research work will include the effect of the induced temperature in drilling FRP composites on the bearing strength of the specimens.

Acknowledgments

This project was supported by the National Science, Technology, and Innovation Plan (NSTIP) strategic technologies program in the Kingdom of Saudi Arabia under grant number 15-ADV4307-03. The authors also acknowledge, with thanks, the Manufacturing &Production Unit, King Abdulaziz University for their technical support.

References

Agwa, M.A. and Megahed, A.A. (2019), "New nonlinear regression modeling and multi-objective optimization of cutting parameters in drilling of GFRE composites to minimize delamination", *Polym. Test.*, **75**, 192-204. https://doi.org/10.1016/j.polymertesting.2019.02.011.

Achache, H., Benzerdjeb, A., Mehidi, A., Boutabout, B. and Ouinas, D. (2017), "Delamination of a composite laminated under monotonic loading", *Struct. Eng. Mech*., **63**(5), 597-605. https://doi.org/10.12989/sem.2017.63.5.597.

Almitani, K.H., Abdelrahman, A.A. and Eltaher, M.A. (2020), "Stability of perforated nanobeams incorporating surface energy effects", *Steel Compos. Struct.*, **35**(4), 555-566. https://doi.org/10.12989/scs.2020.35.4.555.

Baraheni, M., Tabatabaeian, A., Amini, S. and Ghasemi, A.R. (2019), "Parametric analysis of delamination in GFRP composite profiles by performing rotary ultrasonic drilling approach: experimental and statistical study", *Compos. Part B: Eng.*, **172**, 612-620. https://doi.org/10.1016/j.compositesb.2019.05.057.

Beylergil, B., Tanoglu, M. and Aktas, E. (2019), "Mode-I fracture toughness of carbon fiber/epoxy composites interleaved by aramid nonwoven veils", *Steel Compos. Struct.*, **31**(2), 113-123. https://doi.org/10.12989/scs.2019.31.2.113.

Bin Kamisan, M.A.A., Yokota, K., Ueno, T., Kinoshita, H., Homma, S., Yajima, Y. and Takano, N. (2016), "Drilling force and speed for mandibular trabecular bone in oral implant surgery", *Biomater. Biomech. Bioeng.*, **3**(1), 15-26. https://doi.org/10.12989/bme.2016.3.1.015.

Biswal, M., Sahu, S.K., Asha, A.V. and Nanda, N. (2016), "Hygrothermal effects on buckling of composite shell-experimental and FEM results", *Steel Compos. Struct.*, **22**(6), 1445-1463. https://doi.org/10.12989/scs.2016.22.6.1445.

Bhat, R., Mohan, N., Sharma, S., Agarwal, R.A., Rathi, A. and Subudhi, K.A. (2019), "Multi-response optimization of the thrust force, torque and surface roughness in the drilling of glass fiber reinforced polyester composite using GRA-RSM", *Mater. Today: Proceedings*, **19**, 333-338. https://doi.org/10.1016/j.matpr.2019.07.608.

Bui, Q.V. (2011), "A modified Benzeggagh-Kenane fracture criterion for mixed-mode delamination", *J. Compos. Mater.*, **45**(4), 389-413. https://doi.org/10.1177/0021998310376105.

Chandrasekharan, V., Kapoor, S.G. and DeVor, R.E. (1995), "A mechanistic approach to predicting the cutting forces in drilling: with application to fiber-reinforced composite materials", *J. Manufact. Eng. Sci*., **117**(4), 559-570. https://doi.org/10.1115/1.2803534.

Debnath, K. (2019), "Drilling of composite laminates using a special tool point geometry", *In Hole-Making and Drilling Technology for Composites (pp. 63-76)*. Woodhead Publishing. https://doi.org/10.1016/B978-0-08-102397-6.00005-2.

Dehghan, M.S. and Heidary, H. (2020), "Parametric study on drilling of GFRP composite pipe produced by filament winding process in different backup condition", *Compos. Struct.*, **234**, 111661. https://doi.org/10.1016/j.compstruct.2019.111661.

Díaz-Álvarez, A., Díaz-Álvarez, J., Santiuste, C. and Miguelez, M. H. (2019), "Experimental and numerical analysis of the influence of drill point angle when drilling biocomposites", *Compos. Struct.*, **209**, 700-709. https://doi.org/10.1016/j.compstruct.2018.11.018.

Eltaher, M.A. and Mohamed, S.A. (2020), "Buckling and stability analysis of sandwich beams subjected to varying axial loads", *Steel Compos. Struct.*, **34**(2), 241-260. https://doi.org/10.12989/scs.2020.34.2.241.

Eltaher, M.A. and Abdelrahman, A.A. (2020), "Bending behavior of squared cutout nanobeams incorporating surface stress effects", *Steel Compos. Struct.*, **36**(2), 143-161. http://dx.doi.org/10.12989/scs.2020.36.2.143.

Fazilati, J. (2018), "Stability of tow-steered curved panels with geometrical defects using higher order FSM", *Steel Compos. Struct.*, **28**(1), 25-37. https://doi.org/10.12989/scs.2018.28.1.025.

Feito, N., Muñoz-Sánchez, A., Díaz-Álvarez, A. and Miguelez, M. H. (2019), "Multi-objective optimization analysis of cutting parameters when drilling composite materials with special geometry drills", *Compos. Struct.*, **225**, 111187. https://doi.org/10.1016/j.compstruct.2019.111187.

Gemi, L., Morkavuk, S., Köklü, U. and Gemi, D.S. (2019b), "An experimental study on the effects of various drill types on drilling performance of GFRP composite pipes and damage formation", *Compos. Part B: Eng.*, **172**, 186-194. https://doi.org/10.1016/j.compositesb.2019.05.023.

Gemi, L., Köklü, U., Yazman, Ş. and Morkavuk, S. (2020), "The effects of stacking sequence on drilling machinability of filament wound hybrid composite pipes: Part-1 mechanical characterization and drilling tests", *Compos. Part B: Eng.*, **186**, 107787. https://doi.org/10.1016/j.compositesb.2020.107787.

Gemi, L., Morkavuk, S., Köklü, U. and Yazman, Ş. (2020), "The effects of stacking sequence on drilling machinability of filament wound hybrid composite pipes: Part-2 damage analysis and surface quality", *Compos. Struct.*, **235**, 111737. https://doi.org/10.1016/j.compstruct.2019.111737.

Geng, D., Liu, Y., Shao, Z., Lu, Z., Cai, J., Li, X. and Zhang, D. (2019), "Delamination formation, evaluation and suppression during drilling of composite laminates: a review", *Compos. Struct.*, **216**, 168-186. https://doi.org/10.1016/j.compstruct.2019.02.099.

Ghosh, A. and Chakravorty, D. (2019), "Application of FEM on first ply failure of composite hyper shells with various edge conditions", *Steel Compos. Struct.*, **32**(4), 423-441. https://doi.org/10.12989/scs.2019.32.4.423.

Haeger, A., Schoen, G., Lissek, F., Meinhard, D., Kaufeld, M.,

Schneider, G. and Knoblauch, V. (2016), "Non-destructive detection of drilling-induced delamination in CFRP and its effect on mechanical properties", *Procedia Eng.*, **149**, 130-142.

Hamed, M.A., Mohamed, S.A. and Eltaher, M.A. (2020), "Buckling analysis of sandwich beam rested on elastic foundation and subjected to varying axial in-plane loads", *Steel Compos. Struct.*, **34**(1), 75-89. https://doi.org/10.12989/scs.2020.34.1.075.

Heidary, H. and Mehrpouya, M.A. (2019), "Effect of backup plate in drilling of composite laminates, analytical and experimental approaches", *Thin-Wall. Struct.*, **136**, 323-332. https://doi.org/10.1016/j.tws.2018.12.035.

Heidary, H., Mehrpouya, M.A., Saghafi, H. and Minak, G. (2020), "Critical thrust force and feed rate determination in drilling of GFRP laminate with backup plate", *Struct. Eng. Mech.*, **73**(6), 631-640. https://doi.org/10.12989/sem.2020.73.6.631.

Hocheng, H., Chen, C.C. and Tsao, C.C. (2018), "Prediction of critical thrust force for tubular composite in drilling-induced delamination by numerical and experimental analysis", *Compos. Struct.*, **203**, 566-573. https://doi.org/10.1016/j.compstruct.2018.07.051.

Hrechuk, A., Bushlya, V., M'Saoubi, R. and Ståhl, J.E. (2018a), "Experimental investigations into tool wear of drilling CFRP", *Procedia Manufact.*, **25**, 294-301. https://doi.org/10.1016/j.promfg.2018.06.086.

Karimi, N.Z., Heidary, H. and Minak, G. (2016), "Critical thrust and feed prediction models in drilling of composite laminates", *Compos. Struct.*, **148**, 19-26. https://doi.org/10.1016/j.compstruct.2016.03.059.

Kharazan, M., Sadr, M.H. and Kiani, M. (2014), "Delamination growth analysis in composite laminates subjected to low velocity impact", *Steel Compos. Struct.*, **17**(4), 387-403. https://doi.org/10.12989/scs.2014.17.4.387.

Khashaba, U.A. (2004), "Delamination in drilling GFR-thermoset composites", *Compos. Struct.*, **63**(3-4), 313-327. https://doi.org/10.1016/S0263-8223(03)00180-6.

Khashaba, U.A., Seif, M.A. and Elhamid, M.A. (2007), "Drilling analysis of chopped composites", *Compos. Part A: Appl. Sci. Manufact.*, **38**(1), 61-70. https://doi.org/10.1016/j.compositesa.2006.01.020.

Khashaba, U.A. (2013), "Drilling of polymer matrix composites: a review", *J. Compos. Mater.*, **47**(15), 1817-1832. https://doi.org/10.1177/0021998312451609.

Khashaba, U.A., El-Sonbaty, I.A., Selmy, A.I. and Megahed, A.A. (2010), "Machinability analysis in drilling woven GFR/epoxy composites: Part II–Effect of drill wear", *Compos. Part A: Appl. Sci. Manufact.*, **41**(9), 1130-1137. https://doi.org/10.1016/j.compositesa.2010.04.011.

Khashaba, U.A., El-Sonbaty, I.A., Selmy, A.I. and Megahed, A.A. (2013), "Drilling analysis of woven glass fiber-reinforced/epoxy composites", *J. Compos. Mater.*, **47**(2), 191-205. https://doi.org/10.1177/0021998312438620.

Khashaba, U.A. and Khdair, A.I. (2017), "Open hole compressive elastic and strength analysis of CFRE composites for aerospace applications", *Aerosp. Sci. Technol.*, **60**, 96-107. https://doi.org/10.1016/j.ast.2016.10.026.

Khashaba, U.A. and El-Keran, A.A. (2017), "Drilling analysis of thin woven glass-fiber reinforced epoxy composites", *J. Mater. Process. Technol.*, **249**, 415-425. https://doi.org/10.1016/j.jmatprotec.2017.06.011.

Khashaba, U.A. (2020), "Dynamic analysis of scarf adhesive joints in carbon-fiber composites at different temperatures", *AIAA J.*, 1-16. https://doi.org/10.2514/1.J059334.

Khatir, S., Tiachacht, S., Thanh, C.L., Bui, T.Q. and Wahab, M.A. (2019), "Damage assessment in composite laminates using ANN-PSO-IGA and Cornwell indicator", *Compos. Struct.*, **230**, 111509. https://doi.org/10.1016/j.compstruct.2019.111509.

Khatir, S., Boutchicha, D., Le Thanh, C., Tran-Ngoc, H., Nguyen, T. N. and Abdel-Wahab, M. (2020), "Improved ANN technique combined with Jaya algorithm for crack identification in plates using XIGA and experimental analysis", *Theor. Appl. Fract. Mech.*, **107**, 102554. https://doi.org/10.1016/j.tafmec.2020.102554.

Kilickap, E. (2010), "Optimization of cutting parameters on delamination based on Taguchi method during drilling of GFRP composite", *Exp. Syst. Appl.*, **37**(8), 6116-6122. https://doi.org/10.1016/j.eswa.2010.02.023.

Krishnaraj, V., Prabukarthi, A., Ramanathan, A., Elanghovan, N., Kumar, M.S., Zitoune, R. and Davim, J.P. (2012), "Optimization of machining parameters at high speed drilling of carbon fiber reinforced plastic (CFRP) laminates", *Compos. Part B: Eng.*, **43**(4), 1791-1799. https://doi.org/10.1016/j.compositesb.2012.01.007.

Kumar, D., Singh, K.K. and Zitoune, R. (2016), "Experimental investigation of delamination and surface roughness in the drilling of GFRP composite material with different drills", *Adv. Manufact. Polym. Compos. Sci.*, **2**(2), 47-56. https://doi.org/10.1080/20550340.2016.1187434

Liu, D., Tang, Y. and Cong, W.L. (2012), "A review of mechanical drilling for composite laminates", *Compos. Struct.*, **94**(4), 1265-1279. https://doi.org/10.1016/j.compstruct.2011.11.024.

Mahieddine, A., Ouali, M. and Mazouz, A. (2015), "Modeling and simulation of partially delaminated composite beams", *Steel Compos. Struct.*, **18**(5), 1119-1127. https://doi.org/10.12989/scs.2015.18.5.1119.

Melaibari, A., Khoshaim, A.B., Mohamed, S.A. and Eltaher, M.A. (2020), "Static stability and of symmetric and sigmoid functionally graded beam under variable axial load", *Steel Compos. Struct.*, **35**(5), 671-685. https://doi.org/10.12989/scs.2020.35.5.671.

Mishra, P.K., Pradhan, A.K., Pandit, M.K. and Panda, S.K. (2020), "Thermoelastic effect on inter-laminar embedded delamination characteristics in Spar Wingskin Joints made with laminated FRP composites", *Steel Compos. Struct.*, **35**(3), 439. https://doi.org/10.12989/scs.2020.35.3.439.

Moory-Shirbani, M., Sedighi, H.M., Ouakad, H.M. and Najar, F. (2018), "Experimental and mathematical analysis of a piezoelectrically actuated multilayered imperfect microbeam subjected to applied electric potential", *Compos. Struct.*, **184**, 950-960. https://doi.org/10.1016/j.compstruct.2017.10.062.

Mousavi, S.B. and Yazdi, A.A. (2019), "Aeroelastic behavior of nano-composite beam-plates with double delaminations", *Steel Compos. Struct.*, **33**(5), 653-661. https://doi.org/10.12989/scs.2019.33.5.653.

Nguyen, D.H., Bui, T.T., De Roeck, G. and Wahab, M.A. (2019), "Damage detection in Ca-Non Bridge using transmissibility and artificial neural networks", *Struct. Eng. Mech.*, **71**(2), 175-183. DOI: http://dx.doi.org/10.12989/sem.2019.71.2.175.

Ojo, S.O., Ismail, S.O., Paggi, M. and Dhakal, H.N. (2017), "A new analytical critical thrust force model for delamination analysis of laminated composites during drilling operation", *Compos. Part B: Eng.*, **124**, 207-217. https://doi.org/10.1016/j.compositesb.2017.05.039.

Ouagne, P., Ouahbi, T., Park, C.H., Bréard, J. and Saouab, A. (2013), "Continuous measurement of fiber reinforcement permeability in the thickness direction: Experimental technique and validation", *Compos. Part B: Eng.*, **45**(1), 609-618. https://doi.org/10.1016/j.compositesb.2012.06.007.

Ouakad, H.M., Sedighi, H.M. and Younis, M.I. (2017), "One-to-one and three-to-one internal resonances in MEMS shallow arches", *J. Comput. Nonlinear Dynam.*, **12**(5). https://doi.org/10.1115/1.4036815.

Prasad, K.S. and Chaitanya, G. (2019), "Analysis of delamination in drilling of GFRP composites using Taguchi Technique",

Mater. Today: Proceedings, **18**, 3252-3261. https://doi.org/10.1016/j.matpr.2019.07.201.

Phadnis, V.A., Makhdum, F., Roy, A. and Silberschmidt, V.V. (2013), "Drilling in carbon/epoxy composites: experimental investigations and finite element implementation", *Compos. Part A: Appl. Sci. Manufact.*, **47**, 41-51. https://doi.org/10.1016/j.compositesa.2012.11.020.

Rahme, P., Moussa, P., Lachaud, F. and Landon, Y. (2020), "Effect of adding a woven glass ply at the exit of the hole of CFRP laminates on delamination during drilling", https://doi.org/10.1016/j.compositesa.2012.11.020.

Rakesh, P.K., Singh, I. and Kumar, D. (2012), "Drilling of composite laminates with solid and hollow drill point geometries", *J. Compos. Mater.*, **46**(25), 3173-3180. https://doi.org/10.1177/0021998312436997.

Sedighi, H.M., Shirazi, K.H., Noghrehabadi, A.R. and Yildirim, A. H.M.E.T. (2012a), "Asymptotic investigation of buckled beam nonlinear vibration", *Iran J. Sci. Technol. T. Mech. Eng*., **36**(2), 107-116.

Sedighi, H.M. and Shirazi, K.H. (2012b), "Bifurcation analysis in hunting dynamical behavior in a railway bogie: Using novel exact equivalent functions for discontinuous nonlinearities", *Scientia Iranica*, **19**(6), 1493-1501. https://doi.org/10.1016/j.scient.2012.10.028.

Sedighi, H.M. and Daneshmand, F. (2014), "Nonlinear transversely vibrating beams by the homotopy perturbation method with an auxiliary term", *J. Appl. Comput. Mech.*, **1**(1), 1-9. https://doi.org/10.22055/JACM.2014.10545.

Sedighi, H.M., Koochi, A., Daneshmand, F. and Abadyan, M. (2015), "Non-linear dynamic instability of a double-sided nano-bridge considering centrifugal force and rarefied gas flow", *Int. J. Non-linear Mech.*, **77**, 96-106. https://doi.org/10.1016/j.ijnonlinmec.2015.08.002.

Sedighi, H.M. and Bozorgmehri, A. (2016), "Dynamic instability analysis of doubly clamped cylindrical nanowires in the presence of Casimir attraction and surface effects using modified couple stress theory", *Acta Mechanica*, **227**(6), 1575-1591. https://doi.org/10.1007/s00707-016-1562-0.

Taheri-Behrooz, F., Aliha, M.R., Maroofi, M. and Hadizadeh, V. (2018), "Residual stresses measurement in the butt joint welded metals using FSW and TIG methods", *Steel Compos. Struct.*, **28**(6), 759-766. http://dx.doi.org/10.12989/scs.2018.28.6.759.

Tran-Ngoc, H., Khatir, S., De Roeck, G., Bui-Tien, T. and Wahab, M.A. (2019), "An efficient artificial neural network for damage detection in bridges and beam-like structures by improving training parameters using cuckoo search algorithm", *Eng. Struct.*, **199**, 109637. https://doi.org/10.1016/j.engstruct.2019.109637.

Tsao, C.C. and Hocheng, H. (2008), "Evaluation of thrust force and surface roughness in drilling composite material using Taguchi analysis and neural network", *J. Mater. Process. Technol.*, **203**(1-3), 342-348. https://doi.org/10.1016/j.jmatprotec.2006.04.126.

Wang, D.W. and Yin, C.C. (2009), "Detection of edge delamination in surface adhered active fiber composites", *Smart Struct. Syst.*, **5**(6), 633-644. https://doi.org/10.12989/sss.2009.5.6.633.

Xu, Y., Chen, D.M., Zhu, W., Li, G. and Chattopadhyay, A. (2019), "Delamination identification of laminated composite plates using measured mode shapes", *Smart Struct. Syst.*, **23**(2), 195-205. https://doi.org/10.12989/sss.2019.23.2.195.

Yun-Lai, Z.H.O.U. and Wahab, M.A. (2017), "Damage detection using vibration data and dynamic transmissibility ensemble with auto-associative neural network", *Mechanics*, **23**(5), 688-695. https://doi.org/10.5755/j01.mech.23.5.15339.

Zemirline, A., Ouali, M. and Mahieddine, A. (2015), "Dynamic behavior of piezoelectric bimorph beams with a delamination zone", *Steel Compos. Struct.*, **19**(3), 759-776. https://doi.org/10.12989/scs.2015.19.3.759.

CC